Pergamon International Journal of Machine Tools & Manufacture 41 (2001) 1455–1477

INTERNATIONAL JOURNAL OF MACHINE TOOLS & MANUFACTURE DESIGN, RESEARCH AND APPLICATION

Semi-empirical model of surface finish on electrical discharge machining

Kuo-Ming Tsai, Pei-Jen Wang *

Department of Power Mechanical Engineering, National Tsing Hua University, 101 Sec II, Kuang Fu Rd, Hsinchu 30013, Taiwan, ROC

Received 2 September 1999; accepted 11 January 2001

Abstract

A semi-empirical model of surface finish on work for various materials has been established by employing dimensional analysis based upon pertinent process parameters in the electrical discharge machining process. The parameters of the model, such as peak current, pulse duration, electric polarity, and properties of materials, have been initially screened by the design of experiment procedure. Then, they have been systematically analyzed and later verified by making use of the Taguchi method. A model based on dimensional analysis of the model parameters has been established for verification. In addition, the predictions based on the semi-empirical model with the best-fitting parameters by nonlinear optimization methods are in good agreement with the experimental verifications. © 2001 Elsevier Science Ltd. All rights reserved.

Keywords: Semi-empirical model; Surface finish; Electric discharge machining

1. Introduction

Electrical discharge machining (EDM) is currently widely employed for making tools, dies, and other precision parts. In principle, the EDM process is based on the erosive effect of electrical discharges between the tool and the work immersed in a liquid dielectric. Although the exact mechanism of metal erosion during sparking is still debatable, the basic principles of the fundamental theories have suggested that the mechanism is based on a thermal conduction phenomenon governed by heat generated from arc channels and dissipated into the tool and the work. As a result, the work materials near the channels are melted, vaporized, and then flushed off by the

* Corresponding author. Fax: +886-3-572-2840.
E-mail address: pjwang@pme.nthu.edu.tw (P.-J. Wang).

PII: S0890-6955(01)00015-3

dielectric. It has been observed that there are many process variables that affect the surface finish on the work in the EDM process. In previous publications [1–5] it has been reported that the most important variables are level of peak current, duration of current pulse, open voltage of gap, polarity of electrode, thermal properties of the tool, work, and dielectric.

In the EDM process, various empirical models of surface finish have been proposed in the past [6–12]. One of the empirical models based on pulse energy only was suggested by Jeswani [6] and Ghabriel et al. [7]. On the other hand, Osyczka et al. [8] reported four quality models for metal removal rate, tool wear, surface roughness, and power consumed, by employing identification and multi-criteria optimization methods. These four models are dependent on pulse conditions and finished geometry of the tool and work. In addition, some empirical models are based on both peak current and pulse duration [9,10]. However, the models were verified for specific tool materials in combination with various work materials under specific electrode polarity. Pandey and Jilani [11] established specific models for metal removal rate, relative electrode wear, and surface finish based on pulse duration and percentage of cobalt in cemented carbide materials by making use of polynomial regression. While Lee et al. [12] reported that the model of surface finish consisted of peak current and pulse energy. In conclusion, all the above mentioned empirical models considered only pulse conditions for a set of specific tools and work materials under fixed polarity of the electrode. Because the properties of the tool and work materials were neglected, predictions based on all these empirical models were in poor agreement with the experiments.

It should be noted that although an enormous amount of research effort has been put into representing the EDM process by experimental methods, a more elaborate semi-empirical model, based on thermal–mechanical and statistical approaches, has not as yet been reported. In this paper, the objective is to develop a semi-empirical model of surface finish of work for various materials in the EDM process. First, a set of screening experiments were conducted to identify the level of importance of each process parameter, namely peak current, gap open-voltage, pulse on time, pause time, servo voltage (gap control), and electric polarity, for various tool and work materials. The experiments were planned with the help of a design of experiment (DOE) technique, namely the Taguchi method [13,14]. Details of the DOE theory, published in some textbooks, are not described in this paper. Analysis of variance (ANOVA) [13] was used for verifying the screening experiments. Finally, a general semi-empirical model of surface finish based on dimensional analysis of the pertinent process parameters was obtained by making use of optimization methods.

2. Experimental procedure

2.1. Experimental apparatus

A CNC electric discharge machine, Model Mold Maker 3 made by Sodick Inc. in Japan, was used for the experiments. The machine was attached to a MARK XI pulse-charge generator and associated controller to produce rectangular shaped current pulses for discharging purposes. The level of the discharge current was measured with a Hall-effect current sensor, Model HNC-200P made by Nana Electronics Inc. in Japan, which has a built-in voltage amplifier for amplifying the current pulses to the appropriate voltage levels. Both the voltage and the current waveform

on the tool electrode were measured with a digital storage oscilloscope. By looking into the ambient effects, the temperature of the work and the dielectric were monitored by PT-100 temperature probes. During the experiments, an ACL-8112HG data acquisition card, made by Advantech Inc. in Taiwan, attached to a personal computer was used for recording the pertinent signals for all the experiments. In order to control the environment contamination, the dielectric fluid was confined in a stainless-steel container during the experiments. A schematic drawing and photograph of the experimental apparatus are shown in Fig. 1. Before the experiments, all the work samples were ground to the same surface finish. In addition, the surface roughness was measured with a profile-meter, model Hommel Tester T1000 made by Hommelwerke GmbH, Germany.

In the DOE analysis, a statistical software package S-PLUS with DOX module, copyrighted by Statistical Sciences Inc., USA, was used for data analysis [15]. The MATLAB software with Optimization Toolbox [16], copyrighted by MathWork Inc., USA, was employed for optimizing the coefficients of the nonlinear equations in the model.

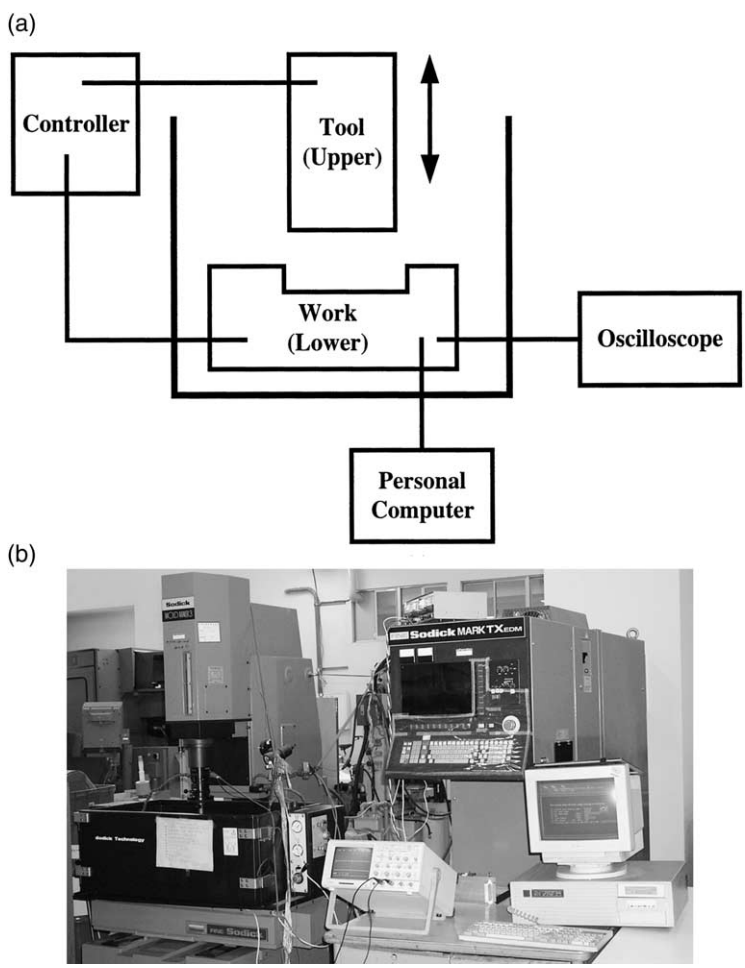

Fig. 1. Schematic drawing and photograph of the experimental apparatus, where (a) is the schematic and (b) is the photograph.

Table 1
Characteristics of the materials in the DOE screening experiments

Materials	Composition	Hardness	Density (kg/m^3)	Surface finish R_{max} (μm)	Mechanical dimension (mm)
Tool					
Cu	>99.95%	HRB 55	8896.6	4.02	ϕ 9.5×50
Gr (ISEM-8)	g-factor 64–70	65 (shore)	1754.5	18.935	ϕ 10×60
Ag-W	W 70%, Ag 30%	HRB 85	14,904.7	3.5	ϕ 10×60
Work					
AISI EK2	C 1.19%, Mn 0.35%, Cr 0.18%	HB179	7809.9	1.42	ϕ 25×13
AISI D2	C 1.52%, Mn 0.34%, Cr 11.29%, Mo 0.71%, V 0.59%	HB217	7723.0	1.47	ϕ 25×13
AISI H13	C 0.43%, Si 1.04%, Mn 0.33%, Mo 1.33%, V 0.98%	HB187	7737.4	1.275	ϕ 25×13

2.2. Materials and design of experiment

In this paper, two levels of experimental work were needed to establish the semi-empirical model. The first level is to identify the importance of the process parameters by screening experiments. At this level, three types of materials, namely copper, graphite, and silver–tungsten alloy, were used for the tool; while three different grades of steel were used for the work. Table 1 shows the pertinent material characteristics and the mechanical dimensions of the tool and the work. Based on the DOE procedures, the pertinent process parameters were selected for further determining the importance level of each parameter, as shown in Table 2, in which the corresponding values of the process parameters are tabulated.

Table 2
Process parameters and levels in the screening experiments

Factors	Symbol	Process parameters	Level		
			1	2	3
Control factor	A (PL)	Polarity of tool	−	+	
	B (ON)	Discharge time (μs)	30	60	120
	C (OFF)	Quiescent time (μs)	30	60	120
	D (Ip)	Peak current (A)	12	30	48
	E (SV)	Servo standard voltage	0	1	2
	F (V)	Main power voltage (V)	60	90	120
	G (An)	Tool materials	Cu	Gr	Ag-W
	H (Ca)	Work materials	EK2	D2	H13
Noise factor	Temp	Temperature of dielectric (°C)	30	50	

Since the importance of the parameters was determined at the first level, an equation consisting of the parameters could be formulated with the help of dimensional analysis. At the second level, more experiments for establishing and verifying the semi-empirical model were needed. It should be noted that pure metals were used for the tool and the work materials because of their traceable physical properties. Therefore, copper and silver were used for the tool, while aluminum, iron, and titanium were used for the work. The mechanical dimensions and pertinent thermal and physical properties of the metals are tabulated in Tables 3 and 4, respectively. In Table 5, the values of the process parameters for the verification experiments based on the materials listed in Tables 3 and 4 are given.

2.3. Screening procedure

The purpose of the screening procedure is to identify the important process parameters in the EDM process. Based on past experiences, there are many parameters that affect the final quality of the work in the EDM process. In this study, the Taguchi method was used to identify the significant parameters in the screening experiments. Six process parameters plus tool and work materials were selected to make the eight controllable parameters in the inner array (i.e. control factors). The outer array (i.e. noise factors) was chosen to be the temperature of the dielectric fluid. Therefore, the inner array is an $L_{18}(2^1\times3^7)$ array and the outer array is an $L_2(2^1)$ array. The $L_{18}(2^1\times3^7)$ array is for the study of the main effect of all the control factors. A block diagram of the screening experiment procedure is shown in Fig. 2, in which the effects of noise factor and control factor and interactions between control factors are completely analyzed. From the results of ANOVA, the important process parameters could be obtained.

It is common practice that the Taguchi method requires both the analysis of the mean response for each run in the inner array and the analysis of variations by using appropriately chosen signal-to-noise ratios (S/N ratio) derived from a quadratic loss function. In the EDM process, the surface finish of the work is a smaller-the-better (STB) quality characteristic. The S/N equation for the smaller-the-better quality characteristic is defined as:

$$\hat{\eta}_S = -10\log\left[\frac{1}{n}\sum_{i=1}^{n} y_i^2\right] \text{(dB)}. \tag{1}$$

Table 3
Characteristics and mechanical dimensions of experimental materials in the second-level experiment

Materials	Composition	Density (kg/m^3)	Surface finish R_{max} (μm)	Dimensions (mm)
Tool				
Cu	>99.95%	8897	4.02	δ 9.5×50
Ag	>99.99%	10,490	5.41	ϕ 10×60
Work				
Fe	>99.9%	7870	1.08	□ 20×12
Al	>99.5%	2699	2.76	□ 20×12
Ti	>99.9%	4507	4.33	ϕ 25×13

Table 4
Pertinent thermal and physical properties of the materials listed in Table 3

Physical property	Unit	Cu	Ag	Al	Fe	Ti	Reference
Density	g/cm^3	8.96	10.5	2.70	7.86	4.51	[17]
Electrical conductivity	$\times 10^5/\Omega$ cm	5.88	6.21	3.65	1.02	0.23	[18]
First ionization energy (remove one	ev[a]	7.724	7.574	5.984	7.87	6.82	[18]
electron)	(kcal/g)[b]	(178)	(175)	(138)	(182)	(158)	
Cathode fall	ev	14.7–15.4	12.1–13.6	17.2–18.6	17.1–18.0	16.8–17.6	[19]
	ev (air)	(8–12)			(8–12)		[20]
	(kcal/g)	(346.8)	(296.1)	(412.5)	(404.4)	(396.4)	
Anode fall	ev[c]	10					
	ev (air)	(2–6)			(2–10)		[20]
	(kcal/g)	(178)	(174.5)	(137.9)	(181.4)	(157.2)	
Work function	ev	4.47	4.28	3.74	4.36	4.09	[21]
	(kcal/g)	(103)	(98.6)	(66.2)	(100.5)	(94.3)	[22]
Thermal conductivity	W/(cm K)	3.98	4.27	2.37	0.803	0.22	[23]
	cal/(s cm K)	0.95	1.020	0.566	0.192	0.055	
Specific heat	cal/(g K)	0.092	0.056	0.215	0.11	0.126	[23]
	cal/(mole K)	(5.846)	(6.041)	(5.801)	(6.143)	(6.035)	
Heat of fusion	kcal/mole	3.11	2.70	2.55	3.67	3.7	[21]
	(kcal/g)	(0.0489)	(0.025)	(0.0945)	(0.0657)	(0.0772)	
Heat of vaporization	kcal/mole	72.8	60.7	67.9	84.6	106.5	[21]
	(kcal/g)	(1.1456)	(0.5627)	(2.5165)	(1.5149)	(2.2233)	
Melting point	K	1356	1233.8	933	1809	1941	[17]
Boiling Point	K	2868	2483	2723	3273	3533	[17]

[a] Ionization potential≈2×Work function.
[b] 1 ev=$(1.60219\times10^{-19}$ (J))/$(1.6606\times10^{-24}$ (g))×1/4.1868 (J)=23.04447231 (kcal/g).
[c] Anode fall≈Ionization potential for gas discharge.

Table 5
Process parameters and corresponding values for the verification experiments

Symbol	Process parameter	Level				
		1	2	3	4	5
PL	Polarity of upper electrode	−	+			
ON	Discharge time (μs)	20	30	60	100	
Ip	Main power peak current (A)	12	22.5	30	39	48
An	Tool materials	Cu	Ag			
Ca	Work materials	Al	Fe	Ti		
OFF	Quiescent time (μs)	60				
V	Main power voltage (V)	90				
SV	Servo standard voltage	2				

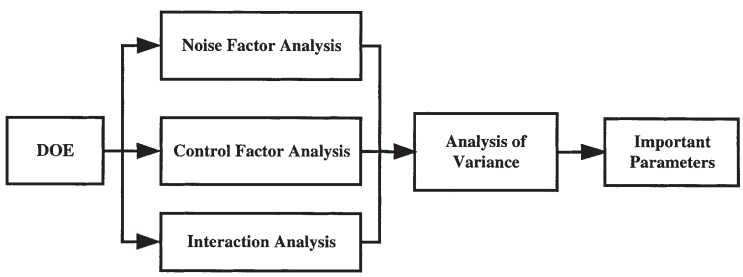

Fig. 2. Procedure block diagram of the screening experiments.

The experimental results of the screening experiment are tabulated in Table 6. One might just need to minimize the surface finish of the work by the listed S/N values.

2.4. Noise factor analysis

Comparisons of the effects of the noise factor, namely the temperature of the dielectric fluid, in the EDM process are illustrated in Table 7. The results indicate that almost no difference exists between the levels of noise factor for the surface finish of work. Therefore, it is concluded that the effects of temperature of the dielectric fluid within the selected temperature range are negligible. The rationale is the temperature rise of the dielectric fluid is much lower than the temperature rise in the discharge channel.

2.5. Control factor analysis

A first-order linear contrast is usually employed for analyzing the linear relationship of the performances and the factors. Similarly, a second-order quadratic contrast can be used to analyze the nonlinear relationship of the performances and the factors, as described in Montgomery's book [13]. With the help of software package S-PLUS, the Pareto plots of S/N contrast on the

Table 6
Experimental results of screening experiments based on the DOE procedure

Exp. No.	Control factor								Surface finish, R_{max} (μm)			S/N (dB)
	A	B	C	D	E	F	G	H	Temp−	Temp+	$\bar{\sigma}$	$\hat{\eta}_S$
1	1	1	1	1	1	1	1	1	11.7	17.2	3.64	−23.35
2	1	1	2	2	2	2	2	2	31.6	31.98	4.58	−30.05
3	1	1	3	3	3	3	3	3	24.04	22.44	2.02	−27.33
4	1	2	1	1	2	2	3	3	15.42	18.65	1.48	−24.67
5	1	2	2	2	3	3	1	1	24.06	21.3	2.74	−27.13
6	1	2	3	3	1	1	2	2	51.5	53.11	4.41	−34.37
7	1	3	1	2	1	3	2	3	52.54	49.97	6.82	−34.20
8	1	3	2	3	2	1	3	1	43.09	40.95	2.73	−32.47
9	1	3	3	1	3	2	1	2	18.09	17.1	1.71	−24.91
10	2	1	1	3	3	2	2	1	29.67	31.11	5.87	−29.66
11	2	1	2	1	1	3	3	2	20.36	19.52	1.39	−26.00
12	2	1	3	2	2	1	1	3	26.32	27.44	2.56	−28.59
13	2	2	1	2	3	1	3	2	36.68	35.65	3.88	−31.17
14	2	2	2	3	1	2	1	3	42.96	38.79	3.41	−32.24
15	2	2	3	1	2	3	2	1	26.09	24.98	3.37	−28.14
16	2	3	1	3	2	3	1	2	59.22	52.44	5.31	−34.95
17	2	3	2	1	3	1	2	3	21.28	26.32	3.32	−27.58
18	2	3	3	2	1	2	3	1	44.2	50.08	5.23	−33.48
Average									32.16	32.17		−29.46
Total average										32.163		

Table 7
Mean response of noise factor, that is the temperature of the dielectric

Level (°C)	Finish, R_{max} (μm)
30	32.16
50	32.17
$\|\Delta\|$	−0.01

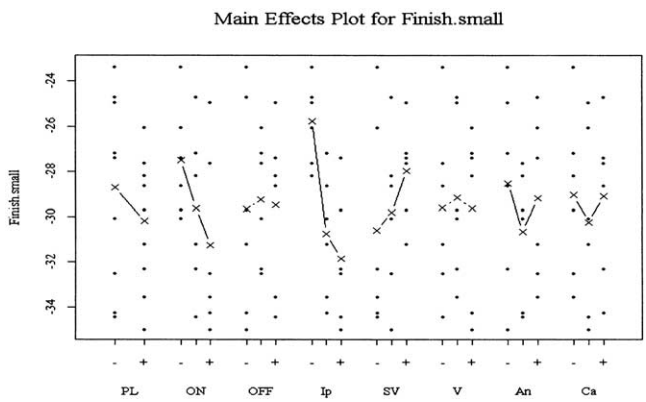

Fig. 3. Response plot for S/N ratio on the surface finish of work where control factors and levels are on the abscissa and the S/N values, in dB, constitute the ordinate.

surface finish of the work were obtained as shown in Figs. 3 and 4. By observing these figures, the significant parameters and their levels are given as follows:

Surface finish: Ip: 1, ON: 1, SV: 3, An: 1, PL: −, Ca: 1. (2)

Although the effect of the servo voltage (SV) is more significant than polarity of work (PL), the

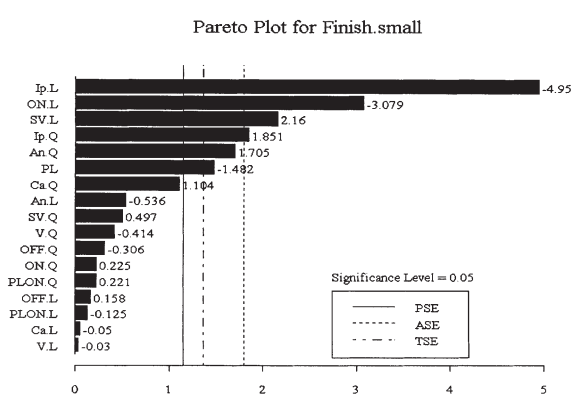

Fig. 4. Pareto plot of factors on the surface finish of work, where the size of effects are on the abscissa and the S/N ratio contrast values, in dB, constitute the ordinate.

Table 8
Response S/N value of PL and ON interactions on surface finish

	$\bar{B}_1$	$\bar{B}_2$	$\bar{B}_3$
$\bar{A}_1$	−26.91	−28.72	−30.53
$\bar{A}_2$	−28.08	−30.52	−32.00

tool materials (An), and work (Ca) materials, the servo voltage was not selected because the voltage is a bearly measurable dynamic value. The effect of polarity of tool and materials of tool are less significant. In practice, it is possible that all work materials are steel alloys with similar physical properties and morphological structure. However, based on the observations in the literature [24,25], the erosive phenomenon of various steel alloys is still quite different. Therefore, the tool and the work materials are very important and should be considered in the semi-empirical model. Finally, five factors including peak current (Ip), discharge time (ON), polarity of work, tool materials, and work materials, were selected as the important parameters for establishing a model of the surface finish.

2.6. PL and ON interaction analysis

The $L_{18}(2^1\times3^7)$ orthogonal array can provide an interaction analysis between columns 1 and 2 of the array without having an effect on the interactions in other columns. Therefore, the values of the interactions between PL and ON on surface finish are shown in Table 8. In addition, it is noted that PL and ON show no interaction (Fig. 5).

2.7. ANOVA

The Taguchi method was originally an intuitive method employed for identifying the important process parameters. Recently, ANOVA has been used to assist the Taguchi method in a more

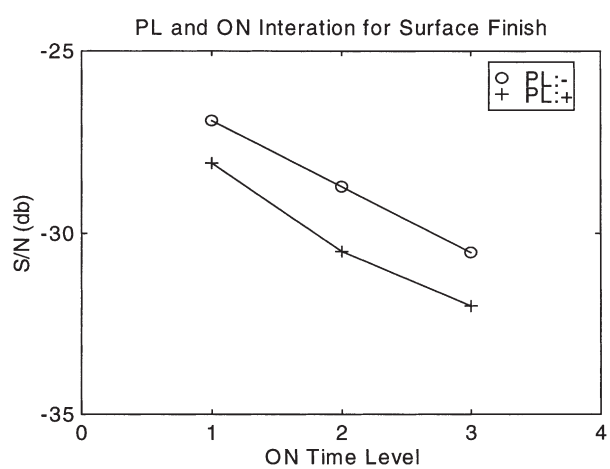

Fig. 5. Plots of PL and ON interactions on surface finish of work.

systematic way. The results of ANOVA are summarized in Table 9, in which parameters such as the polarity of the work, the pulse duration, the peak current, the servo voltage, and the tool materials are significant. These results are in agreement with the results based on the Taguchi method.

3. Dimensional analysis

The Buckingham Π theorem states that it is possible to assemble all variables appearing in a problem into a number of dimensionless products (π_i). In addition, the required relations connecting the individual variables are determined by algebraic expressions relating each π_i [26]. In the previous section, the main factors were identified together with the optimal process conditions and level of surface finish of work, as shown in Eq. (2).

According to the breakdown mechanism of short arc discharge, the dissipated energy in the cathode depends upon the ionization voltage, cathode drop, and work function of the cathode materials. In contrast, the energy dissipated into the anode depends only on the anode voltage drop and the work function of the anode materials [25,27,28]. The effects of electric polarity on electrode erosion can therefore be expressed in terms of the work function, the ionization potential, and the cathode or anode drop, either from the view point of the cathode or the anode. The energy dissipated into the anode and the cathode can be shown as follows:

$$\begin{cases} E \propto V_i + V_c - \varphi & \text{for materials in the cathode} \\ E \propto V_a + \varphi & \text{for materials in the anode.} \end{cases}$$

where V_i is the ionization energy, V_c is the cathode fall, V_a is the anode fall and φ is the work function. In Table 10, eight pertinent physical quantities concerning the energy dissipated into the tool and the work are shown with corresponding dimensions.

As a result, the relationship of surface finish of work can be expressed as follows:

Table 9
ANOVA on the surface finish of work

	Df	SS	MS	F value	Pr(F)[a]
A (PL)	1	9.9756	9.97556	11.03118	0.01051936
B (ON)	2	43.1433	21.57167	23.85440	0.00042527
C (OFF)	2	0.6533	0.32667	–[b]	
D (Ip)	2	125.6233	62.81167	69.45845	0.00000879
E (SV)	2	22.1700	11.08500	12.25802	0.00366411
F (V)	2	0.8100	0.40500	–[b]	
G (An)	2	14.2933	7.14667	7.90293	0.01275334
H (Ca)	2	5.5300	2.76500	–[b]	
Residuals	2	0.2411	0.12056		
(Residuals)	(8)	(7.2344)	(0.90431)		

[a] When Pr(F)<0.05, this indicates that the effect is significant at α=0.05.
[b] The terms are not significant and can be merged to residuals. $F_{0.05}(1,8)=5.32$, $F_{0.05}(2,8)=4.46$.

Table 10
Dimensions of important parameters in EDM process

	Factor	Symbol	Unit	Dimension (MKSA)
Quality characteristic	Surface finish	R_a	μm	L
Parameter	Discharge time	τ_{on}	μs	T
	Peak current	Ip	A	I
	Polarity	PL	–	1
	Input energy onto electrode	E	cal/s	ML^2T^{-3}
Material	Density	ρ	g/cm^3	ML^{-3}
	Electric conductivity	σ	$(\Omega\ \text{cm})^{-1}$	$M^{-1}L^{-3}T^3I^{2a}$
	Specific heat capacity	C_p	cal/(s mole °C)	$L^2T^{-2}\theta^{-1}$
	Thermal conductivity	κ	cal/(mole °C)	$MLT^{-3}\theta^{-1}$
	Melting point	T_m	°C	θ
	Boiling point	T_v	°C	θ
	Latent heat of fusion per unit mass	H_m	cal/g	L^2T^{-2}
	Latent heat of vapor per unit mass	H_v	cal/g	L^2T^{-2}

[a] $\Omega = V/A = \text{m}^2\ \text{kg}\ \text{S}^{-3}\text{A}^{-2}$.

$$R_a = f(I_p, \tau_{on}, E, T_m, T_v, \sigma, C_p, \kappa, \rho, H_m, H_v). \tag{3}$$

For most of the pure metals, it is noted that the value of H_m approximately equals that of $H_v/15$ [29]. Based on a theoretical conjecture, the work metal is removed essentially by evaporation, but a small amount of molten metal remains in the crater. Part of the crater may be ejected owing to the various forces operating in the spark region based on observations in the past [28]. Therefore, it seems justified to assume that the effects of the latent heat of fusion and the melting temperature can be neglected. Hence, Eq. (3) reduces to the following:

$$R_a = f(I_p, \tau_{on}, E, T_v, \sigma, C_p, \kappa, \rho, H_v). \tag{4}$$

Since the dimensionless homogeneous equation of quality characteristics has 10 variables and only five fundamental dimensionless coefficients, the solution can be expressed in the form of a product of five independent dimensionless parts π_s. According to the Buckingham Π theorem, the dimensional formula on the surface finish of work can now be written as:

$$[L]^a[I]^b[T]^c[ML^2T^{-3}]^d[\theta]^e[ML^2T^{-3}I^{-1}]^f[L^2T^{-2}\theta^{-1}]^g[MLT^{-3}\theta^{-1}]^h[ML^{-3}]^i[L^2T^{-2}]^j = [M^0L^0T^0\theta^0I^0]. \tag{5}$$

By equating the powers of the fundamental units on both sides of Eq. (5), a set of simultaneous linear equations are obtained and solved for the constants, with detailed derivations given in Appendix A. The equation on the surface finish of work is given as:

$$R_a = A_1\left[\frac{\alpha}{H_v^{1/2}}\right]\left(\frac{I_p}{\sigma^{1/2}\rho^{1/2}\alpha^{3/2}}\right)^{a_1}\left(\frac{\tau_{on}H_v}{\alpha}\right)^{b_1}\left(\frac{E}{\rho\alpha^2H_v^{1/2}}\right)^{c_1}(J_a)^{d_1}. \tag{6}$$

a_1, b_1, c_1, and d_1 are the power indexes of the corresponding dimensionless brackets in Eq. (6). It should be noted that the thermal diffusivity α of the materials appears with a different power index in all the brackets except J_a.

4. Results and discussions

A semi-empirical model of surface finish of work has been established with model parameters consisting of peak current level, pulse duration, electric polarity, and properties of materials. In addition, a series of experiments, as illustrated in Table 5, have been conducted for verification of the semi-empirical model with different combinations of work and tool materials.

Based on the experimental results, the coefficients and the power indexes in Eq. (6) have been calculated for each work and tool by employing linear and nonlinear regression analysis. In the linear regression analysis, the least square method was chosen. In the nonlinear analysis, four methods, namely the Gauss–Newton, the Davidon–Fletcher–Powell (DFP), the Broyden–Fletcher–Goldfarb–Shanno (BFGS), and the Simplex method were adopted. In both the DFP and BFGS methods, a cubic and a mixed cubic/quadratic polynomial search method were used for the directional search algorithm [30,31]. In Table 11, the final results of the model parameters with copper as the tool and iron/titanium as the work are shown. Also, comparisons on the convergence and effectiveness for the various data-fitting methods are also illustrated. Although the R^2 residues of the linear analysis seem small, the fitted model turned out to be poor when the results of the residual analysis were analyzed. It should be noted that the coefficients and the power indexes in the examples are consistent among the various data-fitting methods. Also, it should be noted that the Gauss–Newton method has the fastest convergence, but the Simplex method has the best stability.

As was mentioned in the literature, the Jacob number (J_a) represents the ratio of sensible heat to latent heat during phase-change of materials in the EDM process [32,33]. Hence, the Jacob number is much dependent on the properties and the microstructure of the work materials. However, if J_a was intentionally neglected in the model in the above cases, the final results would become very poor, as shown in Table 12. This is because the model of surface finish of work is evidently dependent on the properties and microstructure of the work materials. Therefore, J_a is not negligible when various work materials are used for constructing the model. Based on more experimental data, the coefficients and indexes on surface finish of work using a combination of various materials are compared in Table 13. By observing the coefficients and indexes, the results are similar to the results in Table 11. It should be noted that the R^2 values of cases H and I in Table 13 are far from unity. This is because the erosion behavior of titanium is much different from that of aluminum/iron, not only with respect to the thermal, chemical, and physical properties, but also the microstructure. Therefore, the above metals cannot be represented by a single set of coefficients and power indexes. This leads to the conclusion that no single set of coefficients and power indexes exists for various work and tool materials in the EDM process.

Thus, verification of the coefficients and the power indexes of the model have shown very promising results. Therefore, it is of interest to look at further comparisons between the experimental results and predictions based on the model for surface finish of work. Figs. 6–9 show comparisons between the experimental results and the model predictions for surface finish of

Table 11
Coefficients and indexes of the model of surface finish of work obtained by various optimization methods

Optimization method	Linear coefficient	*P*-value	Tool: Cu, work: Fe, Ti					
			Gauss–Newton	DFP (cubic)	DFP (mixed polynomial)	BFGS (cubic)	BFGS (mixed polynomial)	Simplex
Error tolerance			1×10^{-20}	1×10^{-5}	1×10^{-5}	1×10^{-5}	1×10^{-5}	1×10^{-7}
Run time (s)			2.47	4.5	3.02	2.42	3.18	35.43
Epochs			785	66	65	35	70	1105
RMSE[a]			0.556042	0.556042	0.556042	0.556042	0.556042	0.556042
R^2	0.9372 (logistic)		0.855063	0.855063	0.855063	0.855063	0.855063	0.855063
A_1	$e^{13.0301}$	0.0000	$e^{13.9265}$	$e^{13.9265}$	$e^{13.9265}$	$e^{13.9265}$	$e^{13.9265}$	$e^{13.9265}$
a_1	0.4334	0.0000	0.470348	0.470348	0.470348	0.470348	0.470348	0.470348
b_1	0.3168	0.0000	0.287241	0.287241	0.287241	0.287241	0.287241	0.287241
c_1	0.7847	0.0000	0.806976	0.806976	0.806976	0.806976	0.806976	0.806976
d_1	9.2240	0.0000	9.95182	9.95182	9.95182	9.95182	9.95182	9.95182

[a] Root mean squared error.

Table 12
Coefficients and indexes of model of surface finish; Jacob number is neglected

Optimization method	Linear coefficient	*P*-value	Tool: Cu, work: Fe, Ti					
			Gauss–Newton	DFP (cubic)	DFP (mixed polynomial)	BFGS (cubic)	BFGS (mixed polynomial)	Simplex
Error tolerance			1×10^{-20}	1×10^{-5}	1×10^{-5}	1×10^{-5}	1×10^{-5}	1×10^{-7}
Run time (s)			1.7	2.63	2.53	1.81	2.31	20.05
Epochs			550	41	61	27	54	680
RMSE			0.952381	0.952381	0.952381	0.952381	0.952381	0.952381
R^2	0.8391 (logistic)		0.574807	0.574807	0.574807	0.574807	0.574807	0.574807
A_1	$e^{5.2241}$	0.0000	$e^{5.32513}$	$e^{5.32513}$	$e^{5.32513}$	$e^{5.32513}$	$e^{5.32513}$	$e^{5.32513}$
a_1	0.2711	0.0000	0.266003	0.266003	0.266007	0.266003	0.266002	0.266003
b_1	0.2382	0.0000	0.212279	0.212279	0.212273	0.212279	0.212279	0.212279
c_1	0.1974	0.0004	0.193392	0.193392	0.193392	0.193392	0.193392	0.193392

Table 13
Comparisons of model on surface finish with more cases

Case No.	A	B	C	D	E	F	G	H	I
Tool	Cu	Cu	Cu	Ag	Cu Ag	Cu	Cu	Cu	Cu, Ag
Work	Al	Fe	Ti	Ti	Ti	Al, Fe	Fe, Ti	Al, Fe, Ti	Al, Fe, Ti
RMSE	0.37793	0.346788	0.61186	0.526917	0.620949	0.53772	0.556042	1.04113	1.04448
R^2	0.96720	0.948947	0.80052	0.855911	0.797434	0.92757	0.855063	0.693484	0.66583
A_1	$e^{5.83906}$	$e^{-1.02256}$	$e^{-1.41957}$	$e^{-2.40493}$	$e^{-1.83829}$	$e^{-92.8328}$	$e^{13.9265}$	$e^{7.22898}$	$e^{6.76114}$
a_1	0.63855	0.416274	0.54145	0.507217	0.523487	0.56746	0.470348	0.321888	0.31380
b_1	0.32896	0.374538	0.18909	0.249397	0.17763	0.34761	0.287241	0.245281	0.22813
c_1	0.36480	0.868703	0.75672	0.846795	0.794351	0.44793	0.806976	0.081944	0.10368
d_1						−67.0608	9.95182	0.360724	0.20538

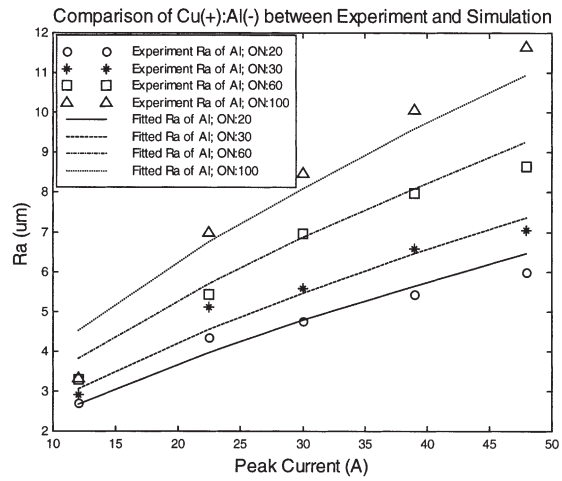

Fig. 6. Comparisons between experimental results and model predictions of the surface finish of work, with Al at the cathode under the process conditions of case A; tool: Cu (+); work: Al (−); average error=6.65%.

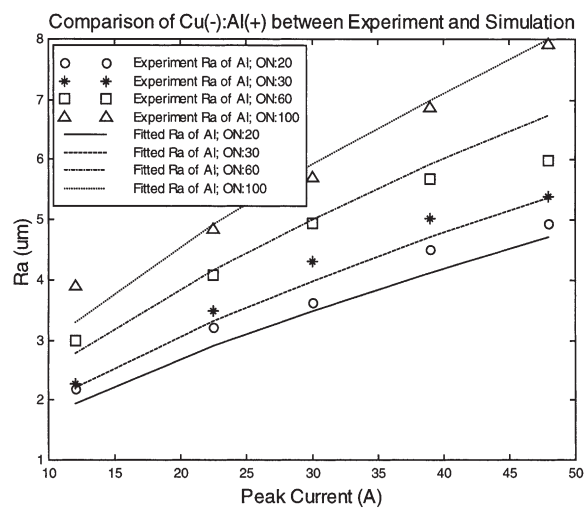

Fig. 7. Comparisons between experimental results and model predictions of the surface finish of work, with Al at the anode under the process conditions of case A; tool: Cu (−); work: Al (+); average error=5.51%.

work, with pertinent process parameters as the abscissa. In these figures, the prediction error is defined as:

$$\text{Error } (\%) = \left| \frac{\text{Experimental results} - \text{Predictions}}{\text{Experimental results}} \right| \times 100\ (\%) \tag{8}$$

From Figs. 6–9, the average prediction errors based on the model are less than 12%. It should be noted that the prediction errors of the model for two of the example cases are small. By

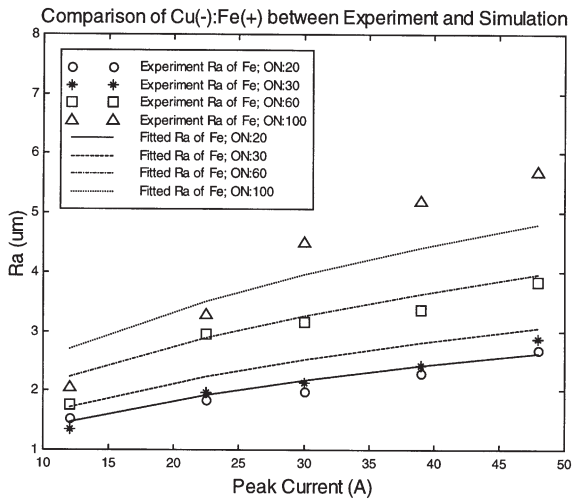

Fig. 8. Comparisons between experimental results and model predictions of the surface finish of work.

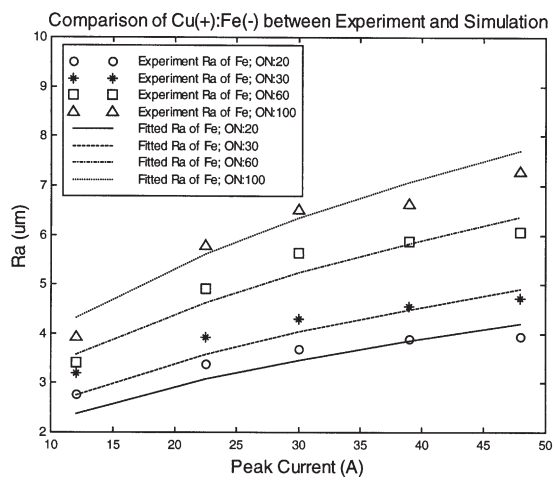

Fig. 9. Comparisons between experimental results and model predictions of the surface finish of work, with Fe at thecathode under the process conditions of case B; tool: Cu (−); work: Fe (+); average error=11.45%.

comparing Figs. 6 and 7 with Figs. 8 and 9, the plots of surface finish versus discharge time under different electrode polarity show the same trends.

In general, predictions of surface finish of work are in reasonable agreement with the experimental results. Therefore, more experimental data within the processing window of the screening experiments were measured and employed for further comparisons between the model of surface finish of work and the tools, as listed in Table 14. In this case the average error between the experiments and the predictions was less than 10%. In conclusion, the model works reasonably well in these verification cases.

Table 14
Comparisons between experimental data and model predictions of surface finish on work[a]

	Conditions	Work material	Surface finish on work			Error (%)
			Experimental R_a (μm)	Predictions R_a (μm)	Differences R_a (μm)	
Model A	Cu(+):Al(−) Ip: 22.5 A; PL: −	Al	5.9675	7.1698	1.2023	20.15
Model A	Cu(−):Al(+) Ip: 22.5 A; PL: +	Al	5.53	5.2317	0.2983	5.39
Model A	Cu(+):Al(−) Ip: 30 A; PL: −	Al	8.5375	8.6157	0.0782	0.92
Model A	Cu(−):Al(+) Ip: 30 A; PL: +	Al	6.7075	6.2867	0.4208	6.27
Model B	Cu(+):Fe(−) Ip: 22.5 A; PL: −	Fe	6.4675	6.0119	0.4556	7.04
Model B	Cu(−):Fe(+) Ip: 22.5 A; PL: +	Fe	3.4675	3.7504	0.2829	8.16
Model B	Cu(+):Fe(−) Ip: 30 A; PL: −	Fe	7.3325	6.7768	0.5557	7.58
Model B	Cu(−):Fe(+) Ip: 30 A; PL: +	Fe	3.89	4.2275	0.3375	8.68
Model C	Cu(+):Ti(−) Ip: 22.5 A; PL: −	Ti	4.195	4.5082	0.3132	7.47
Model C	Cu(−):Ti(+) Ip: 22.5 A; PL: +	Ti	5.34	2.8581	2.4819	46.48
Model C	Cu(+):Ti(−) Ip: 30 A; PL: −	Ti	4.84	5.2681	0.4281	8.85
Model C	Cu(−):Ti(+) Ip: 30 A; PL: +	Ti	4.5625	3.3399	1.2226	26.80
Model D	Ag(+):Ti(−) Ip: 22.5 A; PL: −	Ti	4.09	5.5113	1.4213	34.75
Model D	Ag(−):Ti(+) Ip: 22.5 A; PL: +	Ti	4.9725	3.3095	1.6630	33.44

[a] Other conditions for all the experiments, τ_{on}: 120 μs; τ_{off}: 60 μs; V=120 V.

5. Conclusions

A semi-empirical model of surface finish of work in electrical discharge machining has been established by employing dimensional analysis based on pertinent process parameters such as peak current, pulse duration, electric polarity, and properties of materials. In addition, the parameters of the model have been fitted based on the experimental data generated by the DOE procedures. The final results have shown that the model is dependent on work and tool materials; therefore constant parameters cannot be used for various work and tool materials. According to the best-fitting results on the verification cases, the error analysis shows that the model is reasonably accurate.

Compared to all the empirical models published in the literature, the current semi-empirical

model is mainly based on the thermal, physical, and electrical properties of the work and the tools plus pertinent process parameters. Once the parameters of the model have been determined experimentally for a given work and tool, the model should be able to give reliable predictions under various process conditions. Of course the model is not completely theoretical, but the potential of this model could be further explored if the basic phenomena of the EDM process are better understood in the future.

Appendix A. Derivation of the dimensionless product

The dimensional formula for surface finish of work can be written as:

$$[L]^a[I]^b[T]^c[ML^2T^{-3}][\theta]^e[M^{-1}L^{-3}T^3I^2]^f[L^2T^{-2}\theta^{-1}]^g[MLT^{-3}\theta^{-1}]^h[ML^{-3}]^i[L^2T^{-2}]^j = [M^0L^0T^0\theta^0I^0]. \quad \text{(A1)}$$

By equating the powers of the fundamental units on both sides of Eq. (A1), a set of simultaneous linear equations are obtained which can later be solved to calculate the magnitudes of these constants. The values of the power indexes on the dimensional parameters are listed in Table A1. Based on the homogeneous linear algebraic equations for the dimensions, the coefficients are the numbers in the rows of the dimensional matrix. The simultaneous equations can be written as:

$$\begin{cases} d-f+h+i=0 \\ a+2d-3f+2g+h-3i+2j=0 \\ c-3d+3f-2g-3h-2j=0 \\ e-g-h=0 \\ b+2f=0 \end{cases} . \quad \text{(A2)}$$

Now, rewrite Eq. (A2) into a matrix form,

$$AX=C, \quad \text{(A3)}$$

where

Table A1
Dimensions of parameters on surface finish of work

Index	a	b	c	d	e	f	g	h	i	j
Factor	R_a	I_p	τ_{on}	E	T_v	σ	C_p	κ	ρ	H_v
Dimension										
M	0	0	0	1	0	−1	0	1	1	0
L	1	0	0	2	0	−3	2	1	−3	2
T	0	0	1	−3	0	3	−2	−3	0	−2
θ	0	0	0	0	1	0	−1	−1	0	0
I	0	1	0	0	0	2	0	0	0	0

$$A=\begin{bmatrix} -1 & 0 & 1 & 1 & 0 \\ -3 & 2 & 1 & -3 & 2 \\ 3 & -2 & -3 & 0 & -2 \\ 0 & -1 & -1 & 0 & 0 \\ 2 & 0 & 0 & 0 & 0 \end{bmatrix}, X=\begin{bmatrix} f \\ g \\ h \\ i \\ j \end{bmatrix}.$$

Solving Eq. (A3) for the five independent dimensionless products gives:

1. Assign a=1, b=c=d=e=0 and substitute into Eq. (A3), then

$$C=[0\ -1\ 0\ 0\ 0]^{T}, X=[0\ 1\ -1\ 1\ 1/2]^{T}. \quad \text{(A4)}$$

2. Assign b=1, a=c=d=e=0 and substitute into Eq. (A3) then

$$C=[0\ 0\ 0\ 0\ -1]^{T}, X=[-1/2\ 3/2\ -3/2\ 1\ 0]^{T}. \quad \text{(A5)}$$

3. Assign c=1, a=b=d=e=0 and substitute into Eq. (A3) then

$$C=[0\ 0\ -1\ 0\ 0]^{T}, X=[0\ 1\ -1\ 1\ 1]^{T}. \quad \text{(A6)}$$

4. Assign d=1, a=b=c=e=0 and substitute into Eq. (A3) then

$$C=[-1\ -2\ 3\ 0\ 0]^{T}, X=[0\ 2\ -2\ 1\ -1/2]^{T}. \quad \text{(A7)}$$

5. Assign e=1, a=b=c=d=0 and substitute into Eq. (A3) then

$$C=[0\ 0\ 0\ -1\ 0]^{T}, X=[0\ 1\ 0\ 0\ -1]^{T}. \quad \text{(A8)}$$

The coefficients of the independent dimensionless products are arranged in Table A2. The complete set of dimensionless products is now rewritten as follows:

Table A2
Results of dimensional analysis

	π_1	π_2	τ_3	τ_4	τ_5
a	1	0	0	0	0
b	0	1	0	0	0
c	0	0	1	0	0
d	0	0	0	1	0
e	0	0	0	0	1
f	0	−0.5	0	0	0
g	1	1.5	1	2	1
h	−1	−1.5	−1	−2	0
i	1	1	1	1	0
j	0.5	0	1	−0.5	−1

$$\begin{cases} \pi_1 = \dfrac{R_a C_p \rho H_v^{1/2}}{\kappa} = \dfrac{R_a H_v^{1/2}}{\alpha} \\ \pi_2 = \dfrac{I_p C_p^{3/2} \rho}{\sigma^{1/2} \kappa^{3/2}} = \dfrac{I_p}{\sigma^{1/2} \rho^{1/2} \alpha^{3/2}} \\ \pi_3 = \dfrac{\tau_{on} C_p \rho H_v}{\kappa} = \dfrac{\tau_{on} H_v}{\alpha} \\ \pi_4 = \dfrac{E C_p^2 \rho}{\kappa^2 H_v^{1/2}} = \dfrac{E}{\rho \alpha^2 H_v^{1/2}} \\ \pi_5 = \dfrac{T_v C_p}{H_v} = J_a \end{cases} . \tag{A9}$$

Note that J_a is the Jacob number and $\alpha = \kappa/(\rho C_p)$ is the thermal diffusivity. The relation between the above dimensionless products can now be equated as:

$$\pi_1 = f(\pi_2, \pi_3, \pi_4, \pi_5). \tag{A10}$$

By substituting (A9) into (A10), the complete dimensional equation is as follows:

$$\frac{R_a H_v^{1/2}}{\alpha} = A_1 \left(\frac{I_p}{\sigma^{1/2} \rho^{1/2} \alpha^{3/2}} \right)^{a_1} \left(\frac{\tau_{on} H_v}{\alpha} \right)^{b_1} \left(\frac{E}{\rho \alpha^2 H_v^{1/2}} \right)^{c_1} (J_a)^{d_1} \tag{A11}$$

which can be rewritten as:

$$R_a = A_1 \left(\frac{\alpha}{H_v^{1/2}} \right) \left(\frac{I_p}{\sigma^{1/2} \rho^{1/2} \alpha^{3/2}} \right)^{a_1} \left(\frac{\tau_{on} H_v}{\alpha} \right)^{b_1} \left(\frac{E}{\rho \alpha^2 H_v^{1/2}} \right)^{c_1} (J_a)^{d_1}. \tag{A12}$$

References

[1] H. Cornelissen, R. Snoeys, J.P. Kruth, "Technological surface" — an objective criterion for comparing EDM-systems, Annals of CIRP 27 (1978) 101–106.

[2] A. Erden, D. Temel, Investigation on the use of water as a dielectric liquid in EDM, in: Proceedings of the 22nd International Machine Tool Design and Research Conference, 1981, pp. 437–440.

[3] U.P. Singh, P.P. Miller, W. Urquhart, The influence of EDM parameters on machining characteristics, in: Proceedings of the 25th International Machine Tool Design and Researh Conference, 1984, pp. 337–345.

[4] Y.F. Luo, Z.Y. Zhang, C.Y. Yu, Mirror surface EDM by electric field partially induced, Annals of the CIRP 37 (1988) 179–181.

[5] N. Mohri, N. Saito, Y. Tsunekawa, Metal surface modification by electrical discharge machining with composite electrode, Annals of the CIRP 42 (1993) 219–222.

[6] M.L. Jeswani, Roughness and wear characteristics of spark-eroded surface, Wear 51 (1978) 227–236.

[7] S.R. Ghabriel, S.M. Saleh, A. Kohail, A. Moisan, Problems associated with electrodischarge machined electrochemically machined and ultrasonically machined surfaces, Wear 83 (1982) 275–283.

[8] Osyczka, J. Zimny, J. Zajac, M. Bielut, An approach to identification and multicriterion optimization of EDM process, in: Proceedings of the 23rd International Machine Tool Design and Research Conference, 1982, pp. 291–296.

[9] Iue, Principle of Electric Discharge Machining: Mold Manufacturing Technique, Mihumi Association of Machining Technique, 1983 (in Japanese).
[10] J.H. Zhang, T.C. Lee, W.S. Lau, Study on the electro-discharge machining of a hot pressed aluminum oxide based ceramic, J. Mater. Proc. Tech. 63 (1997) 908–912.
[11] P.C. Pandey, S.T. Jilani, Electrical machining characteristics of cemented carbides, Wear 116 (1987) 77–88.
[12] L.C. Lee, L.C. Lim, V. Narayanan, V.C. Venkatesh, Quantification of surface damage of tool steels after EDM, Int. J. Mach. Tools Manufact. 28 (1988) 359–372.
[13] D.C. Montgomery, Design and Analysis of Experiments (3rd ed.), John Wiley & Sons, 1991.
[14] G.S. Peace, Taguchi Method: A Hands-on Approach, Addison-Wesley, 1993.
[15] MathSoft, S-PLUS for Windows: User's Manual, MathSoft, Inc., Seattle, 1993.
[16] T. Coleman, M.A. Branch, A. Grace, Optimization Toolbox: For Use with MATLAB — User's Guide, Ver. 2, The MathWorks, Inc., 1999.
[17] R.A. Williams, Handbook of the Atomic Elements, Philosophical Library, 1970.
[18] D.E. Gray, American Institute of Physics Handbook, McGraw-Hill, 1963.
[19] C. Kittel, Introduction to Solid State Physics, John Wiley & Sons, 1996.
[20] G.V. Samsonov, Handbook of the Physicochemical Properties of the Elements, Oldbourne, 1968 (translated from Russian).
[21] V.E. Grakov, Cathode fall of an arc discharge in a pure metal I, Soviet Physics–Technical Physics 12 (2) (1967) 286–292.
[22] H.B. Michaelson, Work functions of the elements, J. Appl. Phys. 21 (6) (1950) 536–540.
[23] A. Von Engel, Ionized Gases (2nd ed.), 1965 (Oxford).
[24] I.G. Nekrashevich, S.P. Mitkecich, On some regularities of the phenomena of electric erosion of metals in low-voltage discharges in liquid, Soviet Physics–Technical Physics 1 (1) (1956) 83–88.
[25] F. Van Dijck, Physico-mathematical analysis of the electro discharge machining process, PhD Thesis, Catholic Unversity of Leuven, 1973.
[26] Sedov, Similarity and Dimensional Methods in Mechanics (10th ed.), CRC press, Inc., 1993.
[27] T.H. Lee, T–F theory of electron emission in high-current arc, J. Appl. Phys. 30 (2) (1959) 166–171.
[28] J.D. Cobin, E.E. Burger, Analysis of electrode phenomena in the high-current arc, J. Appl. Phys. 26 (7) (1955) 895–900.
[29] J. Longfellow, J.D. Wood, R.B. Palme, The effects of electrode material properties on the wear ratio in spark-machining, J. Inst. Met. 96 (1968) 614–617.
[30] E. Polak, Optimization: Algorithms and Consistent Approximations, Appl. Math. Sci., vol. 124, Spring-Verlag Inc., New York, 1997.
[31] M.S. Bazara, H.D. Sherali, C.M. Shetty, Nonlinear Programming: Theory And Algorithms, Wiley, New York, 1993.
[32] G.S.H. Lock, Latent Heat Transfer: An Introduction to Fundamentals, Oxford University Press, 1996.
[33] G.F. Hewitt, G.L. Shires, T.R. Bott, Process Heat Transfer, CRC Press, Inc., 1994.